Comparison of Fractal Dimensions of SAR and Optical Digital Elevation Models

Kesavarao, P.,[1] Rao, K. M. M.,[1] and Muralikrishna, I. V.,[2]
[1]Microwave Remote Sensing Data Processing Group, Data Processing Area, National Remote Sensing Centre, Indian Space Research Organization, Balanagar, Hyderabad-500 625, India
E-mail: kesavarao_p@nrsc.gov.in, pkesavarao@gmail.com, kundammrao@gmail.com
[2]Jawaharlal Nehru Technological University, Hyderabad, India, E-mail: iyyanki@gmail.com

Abstract
Digital Elevation Models produced using Radar and Optical image data pairs represent three dimensional complex, irregular shaped topographic surfaces. Since Euclidean Geometry is confined to regular shaped objects, Fractal Geometry is made use of to express the geometrical dimension of DEMs. In this study, Fractal Dimension is computed for Synthetic Aperture Radar (InSAR, SRTM) and Optical (Carto) DEMs by three different approaches viz., Differential Box Counting, Semi-Variogram and Wavelet Power Spectral method. Adequacy of each of the method to compute a single fractal dimension for entire DEM and performance of these methods for SAR and Optical DEM data sets is studied. In case of Variogram method, it is attempted to bring out additional clarity on the technique to identify the extent of linear segment of variogram in order to estimate slope, H and then fractal dimension. The methods are compared and the results are discussed.

1. Introduction

Remote sensing data applications use fractal geometry due to similarities exhibited by the data at different spatial scales. Analogous to spectral, spatial, temporal, angular, and polarization signatures of remote sensing data, fractal engineering has found place in the study of scaling behavior of geographic undulations, roughness indexing, and geometric complexity of irregular terrain surfaces. Euclidean geometry describes topographical dimensions of regular shaped objects whereas fractal geometry is relevant to express the geometry of irregular objects such as coastlines, mountains, clouds, oil spills and DEMs which are complicated to be described by Euclidean geometry. Fractal model is relied on self-similarity or self affinity, which means the fractal objects are scale-invariant and every fractal object can be represented as a rational structured combination of rescaled mini replicas or sub-sets of itself. Since terrain has self similarity characteristics (Martz, 1997 and Li et al., 2006), fractal dimension for DEMs can be estimated. This statistical quantity, helps to infer how completely the fractal fills the space, as one reaches down to smaller and finer scales (Jelinek and Warfel, 2006 and Chen et al., 2007). Fractal geometry deals with the behaviors of sets of points S, in the n-dimensional space $\mathbf{R}^n$, n is an integer and S represents a curve, terrain, image intensity etc. The natural fractal objects are stated to be statistically self-similar and Hausdorff's measure or dimension is used to describe the fractal nature of such objects (Datcua and Seidelb, 1994). Published Literature suggest several ways to estimate the fractal dimension of topographic surfaces, such as the Fractional Brownian model, Triangular prism areas, Box-counting, Differential Box Counting, Projective covering, Blanket method, Area Perimeter, Isarithm, 3D box-counting adaptive method, Hurst exponent method, Variogram or Semi-Variogram, Wavelet Power Spectrum, Wavelet transform of fractal, Jaenisch Method etc (Sun et al., 2006, Chen et al., 2001, Luca et al., 1996, Khalil et al., 2006 and Stark et al., 1997). Out of these methods, Differential Box Counting, Variogram and Wavelet Power Spectra methods are considered in this study as these are noted to be widely used. Fractal dimension values are between 1 and 2 for coastal lines, around 2.5 for surfaces, around 2.7 for urban areas, 1.52 for mean global earth surface and vary between 2 and 3 for DEMs (Luca et al., 1996 and Lam and Quattrochi, 1991). The oil spill patches in sea are discriminated using new formula for fractal box counting by low fractal values of 1.48 to 2.0 for oil spills than look alike and rest of sea surface areas (Marghany et al., 2009). Nature of terrain relief and resolutions are stated to influence the fractal dimensions (Outcalt et al., 1994). The fractal dimensions of different landscapes calculated by different methods are difficult to compare due to limited size of the

regions surveyed and the spatial resolution of DEMs limit the precision and stability of the computed fractal dimension (Xu et al., 1993). Work on estimation of single dimension for entire image to characterize the overall textural complexity of remotely sensed imagery has already been done. Though the application of fractal measurements on conventional DEMs is not new, scope still exists on the study of fractal dimensions on entire digital elevation models derived from various data sources such as SAR and Optical and of large sizes. However, in spite of potential utility of fractal techniques, methodological, step size related, linear segment related concerns have been reported. For example, Variograms do not behave linearly at all scales for topographic surfaces. There is no complete clarity on the extent of linear portion of the variogram to be considered for estimation of slope, though it is mentioned in literature as half or quarter of the length of the maximum record length, and minimum lag vector of one pixel resolution. Another concern seen in literature is on the computational tractability especially when maximum spatial vector length is used due to large volumes of DEM data. It is therefore aimed to bring out some more points to gain more clarity on the extent of linear segments, robustness of the methods on global single fractal dimension estimation, applicability of the methods on DEMs from various sources.

2. Data and Resources used for Study

Twenty SAR DEMs and Ten Carto DEMs are used in this study. Ten InSAR DEMs are generated in house using ERS SAR tandem image pairs (Kesavarao et al, 2010), ten SRTM DEMs are down loaded from internet and all Carto DEMs (Rao KMM, 1994) are used from NRSC data base. SAR and Optical DEMs belong to the same geographical region and the DEMs are customized to suit the study requirements. Geographical areas, DEM array sizes and the horizontal spacing are mentioned here. DEM identification number represents the latitude_longitude_area followed by DEM sizes (pixels x lines). The DEMs used are 135_7925_TPT(1334x1360),1725_78375_HYD(939x1352),17375_78375_HYD(651x1296),1275_775_BLR(1310x1346),1275_77625_BLR(452x1344),12875_775_BLR(1317x1352),12875_77625_BLR(745x1367),2675_76875_JPR(967x1335),26875_7675_JPR(1187x1191), 26875_76875_JPR (1120x1209). InSAR DEMs, SRTM DEMs and Carto DEMs are of 10m horizontal spacing. The DEMs covered plain surface, hilly terrain and elevation values across the DEMs ranged from a minimum of 213m to a maximum of 930 m. The elevation variations within the DEMs ranged from 91m to 673m. One of the generated InSAR DEMs along with corresponding optical and SAR DEMs are shown in Figures 9, 10 and 11. Fractal Dimension is estimated for all thirty such SAR and Optical DEMs using three separate methods. Software is developed in C for estimating fractal dimension using DBC and Variogram approaches. In addition to C programming, Mat lab tool is used for Wavelet Power Spectral method. Computer programs are implemented on Dual CPU quad core Intel processor work stations. Microsoft office 2007 Excel data analysis tool is used for statistical processing and generation of data charts.

2.1 Fractal Dimension by Differential Box Counting

Differential Box Counting is one of the early methods used to estimate the fractal dimension of 3D images (Conci and Monteiro, 2000). If an object of dimension D = 3, is made into, say, three equal segments r = 3, the number of self similar objects or replicas that could be formed will be N = 27 implying $N = r^D$. Thus, the standard equation,

$$D = \frac{\log(N_r)}{\log(1/r)}$$

Equation 1

derived from this principle is adopted, where D represents the Dimension. SAR and Optical DEMs represent elevation or height values 'z' in (x, y) image plane. These DEM data sets of P x P sizes are scaled down to grids of GxG pixels sizes, satisfying the condition $P/2 \geq G > 1$, where step size of the grid G is an integer (Zhang et al., 1999). DEM data of up to 1334 x 1334 pixel array sizes are used in the study. The scaled down GxG grid sizes ranging uniformly from 8 x 8 to 256 x 256 pixels sizes are considered and the ratio r = G / P is derived for all the grid sizes and stored for further computations. On each of these grids, a column of boxes of size G x G x G` exists. If ' h' denotes the height range of the image, G` is given by *[h/G`]=[P/G].* Let the minimum and maximum height values in (i, j)th grid in the DEM, fall in box number 'h_{min}' and 'h_{max}', respectively, then the unit intensity or height cells in a box are expressed by space intensity cells (spicels) or volume pixels (voxels) or simply boxes of above defined dimensions (Chang, 1997). Then $n_r(i, j) = h_{max} - h_{min} + 1$ is the contribution of N_r in (i, j)th grid. Taking all grids in to account, N_r is computed by:

$$N_r = \sum_{i,j} n_r(i,j)$$

Equation 2

For different values of 'r', that is, for different values of G or step sizes from 8 and up to 256, the quantity N_r is determined using an in house developed software program. Then, fractal dimension FD is computed using Richardson log-log plot and by standard least-squares linear fit of **log (N_r) vs log (1/r)** quantities (Sarkar and Chaudhuri, 1994) for all DEMs. One typical representative plot out of thirty such plots is shown in Figure 1. The estimated fractal dimension values for all SAR and Optical DEMs using DBC method are shown in Table 1.

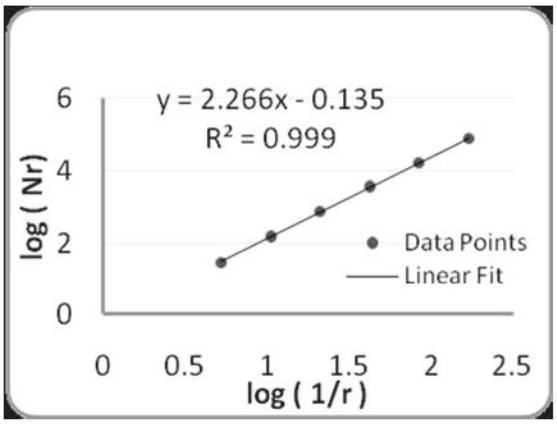

Figure 1: One typical plot of FD for 1725_78375 InSAR by DBC

Table 1: Fractal Dimension and R^2 parameters for SAR and Optical DEMs obtained with three different methods

FD Method→	DBC	DBC	DBC	Vario	Vario	Vario	WPS	WPS	WPS
DEM Source→	SAR		Optical	SAR		Optical	SAR		Optical
DEM Type	InSAR	SRTM	Carto	InSAR	SRTM	Carto	InSAR	SRTM	Carto
DEM ID	FD R^2	FD R^2	FD R^2	FD R^2	FD R^2	FD R^2	FD R^2	FD R^2	FD R^2
135_7925 TPT	2.15 0.999	2.13 1.00	2.22 1.00	2.20 0.998	2.23 0996	2.24 0.996	2.52 0.999	2.52 0.999	2.52 0.999
1725_78375 HYD	2.27 1.000	2.19 0.999	2.31 0.975	2.46 0.987	2.44 0.993	2.49 0.993	2.50 0.999	2.50 0.999	2.50 0.999
17375_78375 HYD	2.33 0.989	2.19 0.999	2.33 0.999	2.50 0.984	2.46 0.998	2.55 0.960	2.49 0.999	2.49 0.999	2.49 0.999
1275_775 BLR	2.16 1.00	2.14 1.00	2.19 1.00	2.36 0.989	2.36 0.990	2.36 0.990	2.52 0.999	2.52 0.999	2.52 0.999
1275_77625 BLR	2.23 0.999	2.13 0.999	2.20 1.00	2.42 0.984	2.41 0.998	2.49 0.991	2.45 0.993	2.59 0.986	2.45 0.993
12875_775 BLR	2.14 1.00	2.05 1.00	2.15 1.00	2.43 0.989	2.39 0.993	2.47 0.995	2.52 0.999	2.52 0.999	2.52 0.999
12875_77625 BLR	2.18 1.00	2.25 0.999	2.17 1.00	2.48 0.991	2.41 0.998	2.54 0.992	2.49 0.999	2.50 0.999	2.49 0.999
2675_76875 JPR	2.31 0.997	2.17 1.00	2.41 1.00	2.82 0.991	2.80 0.950	2.83 0.977	2.49 0.999	2.50 0.999	2.49 0.999
26875_7675 JPR	2.27 0.999	2.22 1.00	2.34 0.999	2.37 0.982	2.41 0.987	2.40 0.983	2.51 0.999	2.52 0.999	2.51 0.999
26875_76875 JPR	2.43 0.993	2.25 1.00	2.38 0.999	2.33 0.983	2.39 0.982	2.4 0.979	2.52 0.999	2.52 0.999	2.52 0.999

2.2 FD by Semi-Variogram

The core of variogram technique is that the statistical variation of elevation between samples is some function of spacing between them (Barnes, 2000, Ehlschlaeger, 2002, Oksanen, 2006, Gloaguen et al., 2007 and Grohmann, 2006). Semivariogram or a Variogram γ ( ), is a function of spatial separation between pixel points (Δ x, Δ y) known as a lag vector, and not a function of the specific location (x, y) in the DEM. If there are say, 'n' elevation values, there will be [n (n-1) /2] unique pairs of elevation values. N (Δ x, Δ y) is the set of all lag vectors, i.e., number of pairs for lag (Δ x, Δ y). For each of these pairs, there is a separation vector. Spatial separation vector of above one resolution cell spacing to a maximum possible vector length are considered with uniform incremental step sizes. In this study, semi variogram is computed by:

$$\gamma(\Delta x, \Delta y) = \frac{1}{2N(\Delta x, \Delta y)} \sum_{(i,j) \in s(\Delta x, \Delta y)} [h_i - h_j]^2$$

Equation 3

h_i , h_j are the elevation values at tail and head of the lag vector. For statistical reasons, the separation or the distance vector is uniformly spaced for of all the DEMs used in this study and the distance classes are evenly spaced in the log–log plot used in the regression. Fractal dimension D, is obtained by, **D =3– H**, where 'H' is Hurst Exponent that represents the surface complexity. **H** is approximated by slope **β** from the linear fit of the variogram using **H = β /2** or **D = 3 – β /2** (Sun et al., 2006 and Xiao, 1997) and linear segmentation scheme is used for estimation of slope. Though the first liner portion having maximum slope is suggested to be taken for estimation of fractal values for all the DEMs (Rees and Muller, 1990 and Burrough, 1981), appropriate linear segment length is arrived at and the details are discussed in results section. Using this method, Varioagrams for all thirty DEMs are computed and fractal dimensions are estimated and shown in Table 1. One typical representative variogram plot out of thirty such variograms, linear segments used for study and R^2 values used to compute the H, FD parameters are reflected in Figures 2 to 6.

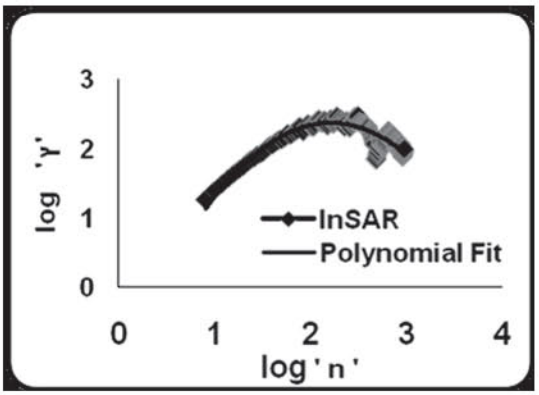

Figure 2: Variogram of 1725_78375 InSAR DEM

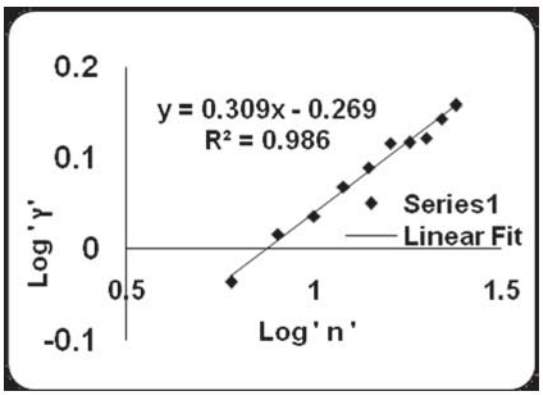

Figure 3: First Linear Segement to estimate H, FD by Variogram

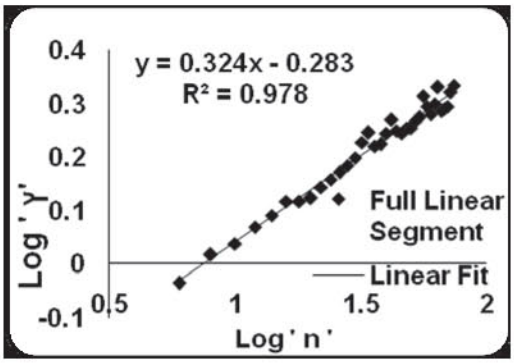

Figure 4: Cumulative Linear Segement to estimate H, FD by Variogram

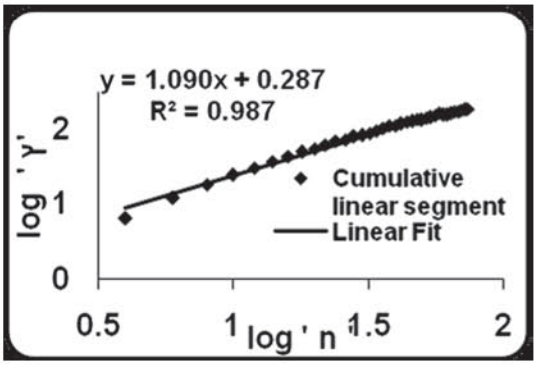

Figure 5: R^2 Values for 1725_78375 InSAR DEM

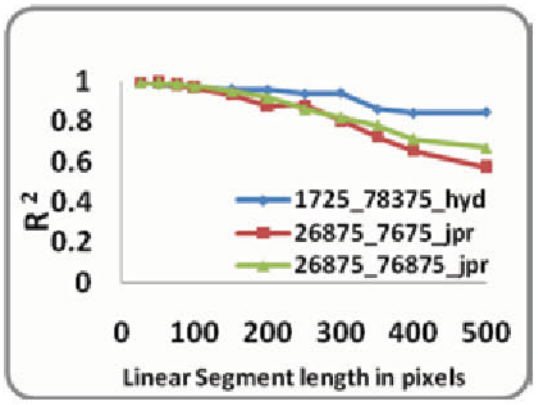

Figure 6: R^2 for various linear segments in variograms for three InSAR DEMs

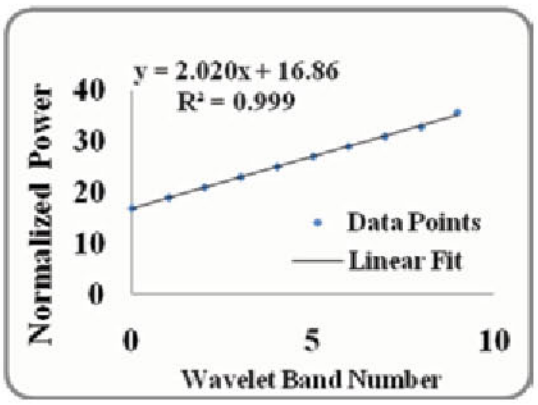

Figure 7: One typical plot of FD estimation for 1725_78375 InSAR using WPS Method

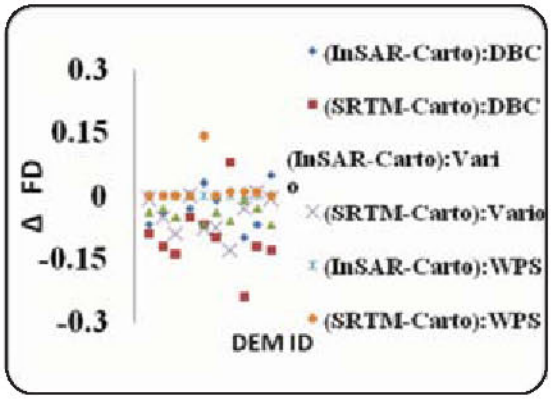

Figure 8: Differences in FD of SAR and Optical DEMs for three methods

Figure 9: BLR_1275_775_CARTO DEM

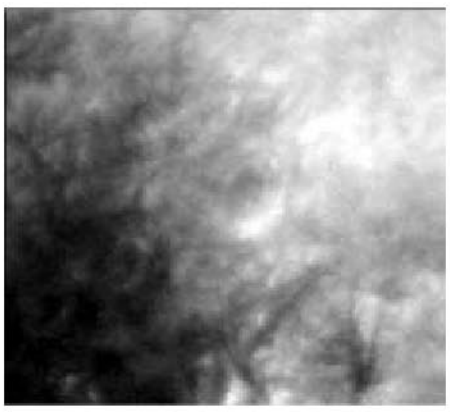

Figure 10: BLR_1275_775_InSAR DEM

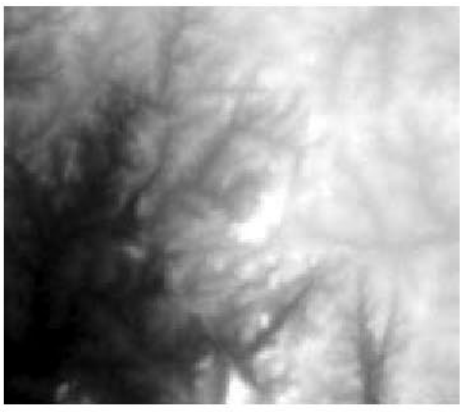

Figure 11: BLR_1275_775_SRTM DEM

Figures 9,10,11: One representative Digital Elevation Model image from each set of Optical, SAR DEMs used in the study along with the DEM Identification Number is shown.

2.3 FD by Wavelet Power Spectrum

In addition to DBC and Variogram methods, wavelet power spectral method is considered to estimate fractal dimensions of DEMs. This method works on the premise that if a signal is similar to itself at different scales, then the wavelet coefficients also will be similar at different scales (Qiawo, 2005). Power law behavior of variance of

wavelet coefficients is made use of to find out the fractal dimensions of all thirty elevation models. Self similarity is global in the sense that scaling laws are expected to hold uniformly at all scales and fractal dimension is not expected to change with time (Flandrin, 1992). Local wavelet power spectrum at a particular decomposition level is calculated by summing up the squares of wavelet coefficients at that level. If there are N elements in a DEM array, where N is a power of two, there will be $\log_2(N)$ coefficient bands or levels or octaves of decomposition for Haar wavelet and one scaling value. That is, power spectrum can be referred as a graphical representation of cumulative information variation at each scale of decomposition. Global wavelet power spectrum is the average of such local power spectra. Two dimensional DEM array elements N, up to 1024 x 1024 which are 2^{10} x 2^{10} array elements are considered in the study. For an N element DEM data set, there will be $\log_2(N)$ wavelet coefficient bands, including the averaging coefficient. The normalized wavelet power spectra for octave *j* is computed using coefficients C_i by:

$$P_j = \frac{1}{2^j} \sum_{j=0}^{2^j-1} C_i^2$$

Equation 4

Since estimation of Hurst exponent requires normalized power, the normalized power is obtained by dividing with 2j. The Hurst exponent is calculated from the slope β of a linear regression line obtained using a set of points (x_j, y_j), where x_j is the octave or band number which is $\log_2$ of band size and y_j is the $\log_2$ of the normalized power. The slope β of this regression line is given by: ***H=[Mod (Slope)-1] / 2*** (Subramani et al., 2006). Large j implies coarser time scales and Regression analysis is sensitive to choice of range (Abry and Veitch, 1998). One typical representative plot out of thirty such plots used for estimation of fractal values using WPS method is given in Figure 7. Differences in FD of SAR and Optical DEMs for three methods are shown in Figure 8.

3. Results

Performance of each of the method on Optical and SAR DEMs is discussed first and then the performance between the methods is reported. Fractal Dimension values computed using DBC method are found to be between 2.05 and 2.43 for SAR DEMs and between 2.15 and 2.41 for Optical Carto DEMs (Luca et al., 1996). At 95% confidence level, the confidence interval for difference in means for Optical and InSAR DEMs is ((2.27-2.247)± 2.26*0.04198)=(0.12,-0.07). The value zero is contained in the interval, indicating 'insignificant difference' in FD values for InSAR DEMs with respect to Optical DEMs at 0.05 confidence level. Similarly, for SRTM and InSAR DEMs, the interval is found to be (0.01,-0.16) and this also indicates insignificant difference in FD values for InSAR DEMs with respect to SRTM DEMs at 0.05 confidence level. Fractal Dimension values estimated using semi variogram method are found to be between 2.20 and 2.50 for SAR DEMs and between 2.24 and 2.54 for Optical Carto DEMs. At 95% confidence level, the confidence interval for difference in means for Optical and InSAR DEMs is (0.20,-0.12). The value zero is included in the interval, indicating 'insignificant difference' in FD values between Optical and InSAR DEMs at 0.05 confidence level. Similarly, between SRTM and InSAR DEMs, the interval is found to be (0.15,-0.16) and this indicates an 'insignificant difference' for InSAR DEMs with respect to SRTM DEMs at 0.05 confidence level. To understand more on the selection of linear segment for estimation of slope, varied linear portions of a few variograms are analyzed. Starting after first resolution cell, linear portions with cumulative increments of 25 pixels distances reaching up to 500 pixel lag vector lengths are considered for estimation of slope, H and then FD values. Since the average 'range of the variograms' is known to be around 350 pixel distance, linear segments stretching up to 500 pixels spacing are considered for the study. It is seen that R^2 of 0.98 and better exists for the first three linear portions extending up to 75 pixel lengths and the correlation falls as lag vector goes to 350 pixel length and becomes poor at 500 pixel spatial distance. From the FD values, it is seen that the cumulative linear segment of up to 75 pixel spatial distance could be considered for estimation of slope from semi variograms, provided R^2 is > 0.98 for the segment under consideration. For WPS method, at 95% confidence, the confidence interval for difference in means for Optical and InSAR DEMs is (0.02,-0.02). The value zero is contained in the interval, indicating 'insignificant difference' for InSAR DEMs with respect to Optical DEMs at 0.05 confidence level. Similarly for SRTM and InSAR DEMs, the interval is found to be (0.01,-0.04) and this indicates an insignificant difference for InSAR DEMs with respect to SRTM DEMs at 0.05 confidence level. In the next step, comparison is made between the methods for InSAR DEMs and repeated for Optical DEMs. Inter comparison between methods revealed that the FD values from variogrm and WPS methods are higher by around 0.2 and 0.3 respectively with respect to values obtained by DBC which agrees well with the

Lam, N. S. N., and Quattrochi, D. A., 1992, On the Issues of Scale, Resolution, and Fractal Analysis in the Mapping Sciences, Professional Geographer, Association of American Geographers, 88-98.

Luca, D., Datcu, M., and Seidel, K., 1996, Multi resolution Analysis of DEMs: Error and Artifact Characterization, RSL, ESA, Fringe.

Li, L., Sun, C., and Du, Q., 2006, A New Box-Counting Method for Estimation of Image Fractal Dimension, IEEE, 3029-3032.

Marghany, M., Cracknell, A., and Hashim, M., 2009, Modification of Fractal Algorithm for Oil Spill Detection from RADARSAT-1 SAR Data, *International Journal of A.E.O.G.,* 5 (11), 96-102.

Marghany, M., Cracknell, A., and Hashim, M., 2009, Comparison between Radarsat-1 SAR Different Data Modes for Oil Spill Detection by a Fractal Box Counting Algorithm. *Intl. Jl. of Digital Earth*, 2 (3), 237-256.

Oksanen, J., 2006, Digital Elevation Model Error in Terrain Analysis, Academic Dissertation in Geography, Doctoral Dissetation, University of Helsinki, Finland.

Outcalt, S. I., Hinkel, K. M., and Nelson, F. E., 1994, Physiography, *Geomorphology,* 11, 91-106.

Rao, K. M. M., 1994, Terrain Analysis and Perspective Views Generation from Digital Terrain Model" - ICORG seminar, JNTUH.

Rees, D., and Muller, J. P., 1990, Surface Roughness Estimation using Fractal Variogram Analysis, Geoscience and Remote Sensing Symposium, *IGARSS* 90, 1951-1954.

Qiawo, F., 2005, Workshop 118 on Wavelet Application in Transportation Engineering", Texas Southern University.

Sarkar, N., and Chaudhuri, B. B., 1994, An Efficient Differential Box-Counting Approach to Compute Fractal Dimension of Image, *IEEE Transactions on Systems, Main and Cybernetics*, Vol 24, No. 1, 115-120.

Stark, B., Adams, M., Hathaway, D. H., and Hagyard, M. J., 1997, Evaluation of two Fractal Methods for Magneto Gram Image Analysis, Solar Physics174: 297–309, Kluwer Academic Publishers, Belgium.

Sun, W., Xu, G., Gong, P., and Liang, S., 2006, Fractal Analysis of Remotely Sensed Images: A Review of Methods and Applications, *International Journal of Remote Sensing*, Vol. 27, No. 22, 4963–4990.

Subramani, P., Sahu, R., and Verma, S., 2006, Feature selection using Haar Wavelet Power Spectrum, *BMC Bioinformatics*, Vol. 7.

Xiao, Y., 1997, Topographic Characteriza -tion for DEM Error Modeling, PhD Thesis, Canada.

Xu, T., Moore, I. D., and Gallant, J. C., 1993, Fractals, Fractal Dimensions and Landscapes — A Review, *Geomorphology*, Vol. 8, Issue 4, 245-262.

Zhang, Z. Y., Drake, N. A., Wainwright, J., and Mulligan, M., 1999, Comparison of Slope Estimates from Low Resolution Dems: Scaling Issues and a Fractal Method for Their Solution, Earth Surface Processes and Landforms Earth Surf. Process. *Landform.s* 24, 763-779.